Chemical ordering in magnetic FePd/Pd(001) epitaxial thin films induced by annealing

D. Halley,[1,*] B. Gilles,[2] P. Bayle-Guillemaud,[1] R. Arenal,[1] A. Marty,[1] G. Patrat,[3] and Y. Samson[1]
[1]*CEA Grenoble, Département de Recherche Fondamentale sur la Matière Condensée, Service de Physique des Matériaux et Microstructures, 17 avenue des Martyrs, 38054 Grenoble Cedex 9, France*
[2]*CNRS/LTPCM, ENSEEG, BP 75, 38045 Grenoble, France*
[3]*CNRS/laboratoire de cristallographie, BP 166, 38042 Grenoble, France*
(Received 19 February 2004; published 18 November 2004)

Chemically disordered FePd epitaxial layers are grown at room temperature by molecular beam epitaxy on a Pd(001) buffer layer and then annealed in order to induce the chemically ordered $L1_0$ (AuCu I) structure. Contrary to what is observed in the case of ordering during growth above room temperature, the ordered structure appears here with the three possible variants of the $L1_0$ phase. The ratio of the three different variant volumes is set by the residual epitaxial strain in the layer before annealing. It thus explains that for long annealing times, the long-range order parameter associated with the $L1_0$ variant with *c* along the (100) growth direction saturates at a value close to 0.65, and never reaches unity. Magnetic consequences of the ordering are studied.

DOI: 10.1103/PhysRevB.70.174437 PACS number(s): 75.10.Hk, 61.10.Nz, 68.37.Lp, 61.72.Nn

I. INTRODUCTION

The chemical ordering of metallic alloys is a problem of wide interest, concerning for instance the magnetic properties associated with some ordered alloy phases [FePt,[1] FePd (Refs. 2–4)] or the change in plastic properties with chemically ordered structures.[5] Much attention has been recently paid to two important parameters that can influence the ordering of metallic alloys in thin films: first, the strain, due to the epitaxial relationship between the layer and the substrate, may promote metastable phase[6,7] that are not observed in bulk phases and second, the symmetry breaking due to the surface can play a drastic role and drive the chemical ordering. This has been thoroughly studied, for instance by Barbier *et al.*[8] and Legoff[9] in the case of $L1_2$ ordered CuPd alloys upon annealing.

FePd belongs to the metallic alloys that are widely studied because of their large magnetic anisotropy along the quadratic axis in the $L1_0$ chemically ordered structure (Fig. 1), as for FePt (Ref. 1) and CoPt (Refs. 10 and 11) alloys. Following the phase diagram[12] there is indeed a $L1_0$ phase for temperatures below 650 °C near the $Fe_{0.5}Pd_{0.5}$ composition. This structure is slightly tetragonal contrary to the chemically disordered structure (γ phase) that is purely fcc. Three possible variants are hence possible within this $L1_0$ structure, with the quadratic *c* axis along one of the three $\langle 100 \rangle$ directions in the cubic structure. For the sake of simplicity, in the case of thin films grown on Pd(001), we will call *Z* the variant with *c* along [001] and *X* (resp. *Y*), those with *c* along [100] (resp. [010]). The chemical ordering of the alloy during growth has been shown[13–15] to depend strongly on the substrate temperature in the case of molecular beam epitaxy (MBE) deposition. If they are grown above 350 °C, layers grown by codeposition of Fe and Pd order almost perfectly and exhibit just the *Z* variant of the $L1_0$ structure, i.e., the *c* axis and the associated magnetic anisotropy are perpendicular to the plane of the film. It has been claimed[7] that the biaxial tensile strain due to epitaxial misfit greatly favored the selection of the observed *Z* variant and thus was the key to understand the FePd ordering. In fact, it has been recently suggested that this ordering was mostly driven by diffusion of Pd adatoms at the surface—respectively, of Pt adatoms in FePt-,—during growth[1,13] and that this would hence explain the selection of variant with *c* parallel to the growth direction.

We here aim at studying post-growth ordered samples to make a comparison with films ordered during growth and, by this way, to highlight the role plaid by the surface in both cases. We study by x-ray diffraction (XRD) and transmission electron microscopy (TEM) the effect of post-growth annealing at 400 °C of disordered samples as a function of time. We observe the size and shape of the different variant domains of the $L1_0$ phase as well as the chemical long-range order (LRO) parameter related to the different variants. We suggest a stress-driven control of the proportion of the different variant domains, contrary to the case of films ordered during epitaxial films. We also investigate the magnetic con-

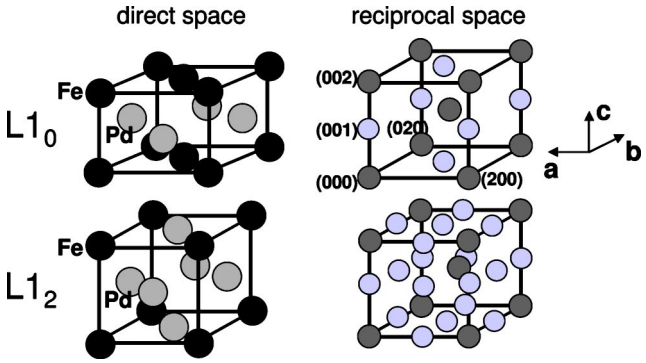

FIG. 1. FePd unit cells in the $L1_0$ and $L1_2$ chemically ordered structures with the associated superstructure spots in the reciprocal space. *C* is the tetragonal axis in the $L1_0$ structure. The $L1_2$ structure is cubic.

sequences of this three-variant ordering of the FePd thin film by measuring hysteresis loops by extraordinary Hall effect and by vibrating sample magnetometry (VSM).

II. GROWTH AND ANNEALING

Bulk MgO(001) crystals provided by Earth Chemical (Japan) were used as substrates for the epitaxial growth. They were first degreased by successive baths in trichloroethane, acetone, and methyl alcohol and next introduced in a UHV-preparation chamber. There, they were annealed during six hours up to 550 °C so as to obtain a clean surface. The growth of the 70 nm Pd buffer was performed at room temperature on a 3 nm Cr seed layer. Once grown, the buffer was annealed at 450 °C during 15 min to smooth the Pd(001) surface. The Pd and Fe fluxes from the electron beam evaporators were then measured using the reflection high-energy electron diffraction (RHEED) intensity oscillations corresponding to the growth of pure Pd and of FePd alloy at room temperature on a Pd(001) sample. Thereafter, Fe and Pd fluxes were both set to 0.16 monolayer (ML) per second and maintained constant by using the indications of two quartz microbalances. The growth of the FePd layer was next performed by simultaneous evaporation of both elements on the Pd(001) substrate held at room temperature. The film thickness was 40 nm. The pressure remained in the low 10^{-7} Pa range.

Annealings were performed *in situ* in an adjacent chamber under ultra high vacuum (in the 10^{-8} Pa range). Before removing the sample from the chamber, a 2 nm Pd capping layer was deposited on top in order to prevent the film from oxidation in air.

First, let us remind the main results[4,13–16] we already obtained concerning films grown by codeposition: FePd films grown at room temperature are disordered and the 2.3% tensile epitaxial misfit ($a_{\text{disordered FePd}}=3.80$ Å and $a_{\text{Pd}}=3.89$ Å) is relaxed by $\frac{1}{2}$ [101] perfect dislocations at the FePd/Pd interface. On the contrary, when the growth is performed at higher temperature (above 350 °C), the films are well $L1_0$ ordered with c along the growth direction [001] (Z variant). In this case, the related long-range order parameter (LRO) (see below) is close to 0.8. The 1% misfit ($a_{a,b}=3.85$ Å, $a_c=3.71$ Å) is relaxed by 1/6 [112] perfect dislocations which pile up in microtwins. No X or Y variants are in that case observed.

III. X-RAY DIFFRACTION

XRD measurements were performed with a classical θ–2θ homemade diffractometer working with a Cu anode. As-deposited films do not show (001) and (003) reflections on θ–2θ scans: they are forbidden in the fcc symmetry of the FePd in the disordered γ phase. After a few hours annealing at 400 °C, these extra reflections appear [Fig. 2(a)], showing the onset of $L1_0$ ordering. These two superstructure peaks are associated with the Z variant only.

We define the $L1_0$ LRO parameter of FePd related to the Z variant as $S_Z=|n_{\text{Fe}}-n_{\text{Pd}}|$ where n_{Fe} (resp. n_{Pd}) is the probability of finding a Fe atom on the Fe $L1_0$ sublattice (resp. on the Pd $L1_0$ sublattice) corresponding to the Z variant. This S_Z value is calculated from the ratio of the integrated intensities of the (001) and (003) superstructure peaks versus the (002) and (004) fundamental peaks[2,4,16–18] [Fig. 2(b)]. It may vary between 1 for the perfectly ordered alloy with only the Z variant and 0 for the fully disordered alloy. Figure 2(c) shows the increase of S_Z with the annealing time for different samples grown in the same way and annealed at 400 °C. The LRO parameter seems to saturate at a value close to 0.65 after long annealing. As we only take into account one of the

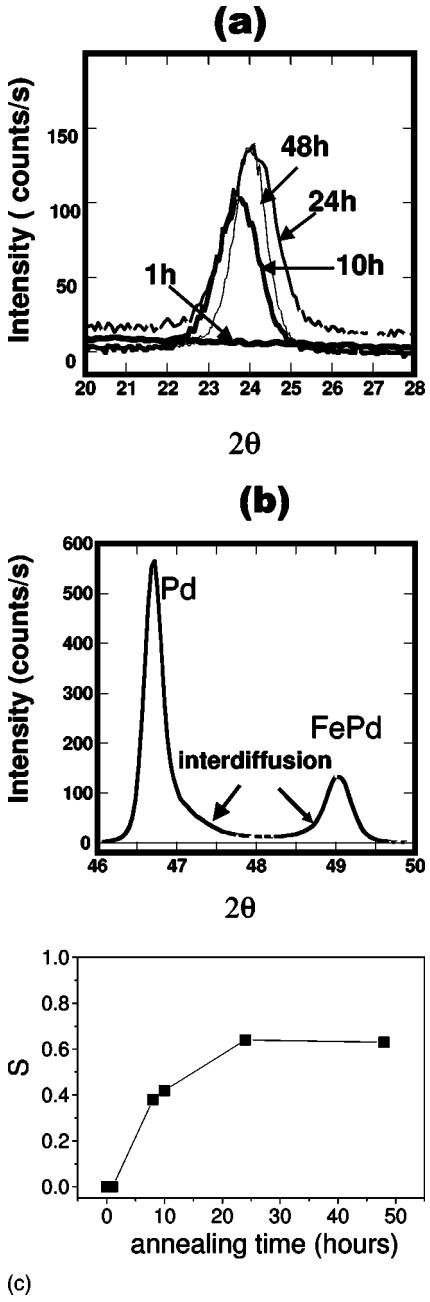

FIG. 2. (a) θ-2θ x-ray diffraction scans on FePd films after different annealing times at 400 °C; spectra are normalized on the Pd(002) peak (b) θ-2θ scan on Pd(002) and FePd (002) after 48 h anneal at 400 °C. The shoulders on both peaks show the diffusion of iron into the Pd buffer layer. (c) Long-range order parameter (S) on the same samples as for (a) as a function of annealing times.

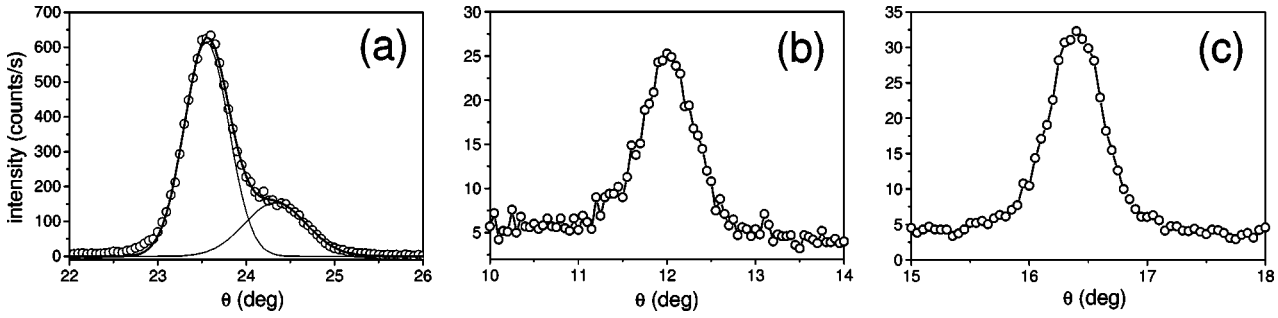

FIG. 3. In plane X-Ray diffraction: ϕ-2θ scans on a FePd sample annealed at 400 °C for 24 h. (a) (200) peak fitted with two Gaussian contributions due to the *X* variants on the one hand and to the *Y* and *Z* variants on the other hand; (b) (100) peak associated to the *X* variant; (c) (110) peak associated to the *Z* variant.

three $L1_0$ variants (the one with *c* along [001]) in the calculation of S_Z, we can make two assumptions to explain this saturation: either the volume occupied by the perfectly ordered *Z* variant is limited and corresponds to a fraction of the total volume of FePd or the film is homogenously and nonperfectly ordered along [001] with a constant LRO parameter of 0.65 in the whole FePd layer.

Moreover, it may be noticed that the crystalline quality increases after annealing for 48 h: The mosaicity decreases from about 1.4° to less than 0.7°. Also, the lateral size of the ordered domains, deduced from the full width at half maximum of the (001) and (003) peaks obtained on rocking curves is in the order of 120 Å. The measurements made on the (113) and (002) FePd peaks indicate a lattice parameter of 3.71 ± 0.005 Å in the out-of-plane direction and 3.82 ± 0.005 Å in the in-plane direction. Therefore, the structure is not yet completely relaxed ($a_{\text{in-plane}} = 3.85$ Å is expected if completely relaxed with the *Z* variant). A shoulder may be observed [Fig. 2(b)] on the right side of the θ–2θ scans on the FePd (002) and on the Pd (002) peaks, corresponding to the diffusion of Fe into the Pd buffer during annealing, that will be discussed later.

In order to check the presence of in-plane variants of the $L1_0$ FePd (*X* and *Y* variants), we tried to observe the associated (103) and (013) reflections: The intensity on these peaks is yet too low to be measured. We thus performed in-plane diffraction measurements, using the grazing incident diffraction technique, to have access to the more intense (100) and (010) reflections that are related to *X* and *Y* variants. In this technique, both the incoming and outcoming beams make a grazing angle with the surface and the Bragg conditions are fulfilled by planes perpendicular to the surface.[19] ϕ is the angle between the incident beam and the diffracting planes normal. Figure 3 clearly shows these peaks on ϕ–2θ scans, thus proving the presence of the two in-plane variants. The (200) and (400) peaks exhibit a shoulder and can be fitted with two contributions: The main one corresponds to an in-plane lattice parameter of 3.85 Å and the other one with an in-plane lattice parameter of 3.76 Å. The larger lattice may be related to the *Z* and *Y* variant whereas the smaller one may be related to the *X* variant. The latter lattice parameter corresponding to *X* domains is larger than expected from then bulk (3.71 Å). This will be explained below. From the ratio of the two components of the fit on the (200) and (400) reflections we deduce that the volume associated with the *X* variant is about 1/6 of the total volume. The same 1/6 proportion was observed on the symmetrical *Y* variant, thus suggesting that the *Z* variant occupies the majority of the volume (about 2/3).

We performed the integration by ϕ scans of the (100), (300), (110), (200), (400), and (220) peaks. We used widely open slits in front of the detector in order to integrate the whole peak. In the case of the fundamental (200) and (400) peaks we therefore do not discriminate between the contributions of the different variants. It means that the LRO parameter we obtain is related to the whole volume of the FePd film, even if it is in fact due to a limited volume of this layer (*X*, *Y*, or *Z* domains). From this, we obtained LRO parameters: $S_z = 0.66$ for the *Z* variant and $S_x = 0.29$ for the *X* variant. The first value is consistent with the value obtained from θ–2θ scans ($S_Z = 0.65$) (see above). These values can be normalized with respect to the related volume of each variant if we suppose that the intensity of the superstructure peaks is proportional to the volume of domains corresponding to the involved variant.

$I_{\text{superstructure}} \propto V_{\text{total}} (S_i)^2 = V_i (S_i^{\text{local}})^2$, where S_i^{local} is the local LRO parameter (within a given domain) and V_i is the volume of domains ordered with this variant *i* (*i*=*X*, *Y*, or *Z*). With $V_{x,y} = 1/6$ and $V_z = 2/3$ this leads to $S_z^{\text{local}} = 0.81$ and $S_x^{\text{local}} = 0.71$. These values are relatively close to 1 and thus show a high $L1_0$ ordering within the different variant domains. The error bars on the S_i values can be assessed at 0.1–0.15, due to experimental inaccuracies and to the extra contribution of the small $L1_2$ interdiffusion zone (see below) to the superstructure peaks of FePd.

IV. TRANSMISSION ELECTRON MICROSCOPY (TEM) AND ELECTRON ENERGY LOSS SPECTROSCOPY (EELS)

We performed TEM cross sections and plane view observations using a 400 kV JEOL 4000EX. The samples were prepared using mechanical polishing and Ar^+ ion milling. Figure 4 shows a (100) cross section of a FePd layer after 48 h annealing at 400 °C. The two dark field images made with the (001) and the (100) reflections show complementary domains for the two corresponding *X* and *Z* variants. As may be seen, the in-plane ordered domains [variant *X* associated with the (100) reflection] form thin (3–5 nm wide) prisms

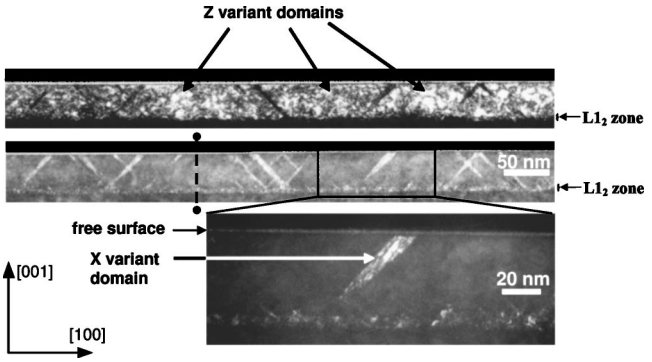

FIG. 4. TEM cross section along (010) (zone axis [010]) on a 40 nm FePd layer annealed at 400 °C for 48 h. Dark field images on (001) spot (top) and on (100) spot (bottom), showing, respectively, the complementary *Z* and *X* variants domains, and for both spots the $L1_2$ interfacial region. A zoom on a *X*-variant domain is given, also showing some APB (dark lines within the *X*-variant domain).

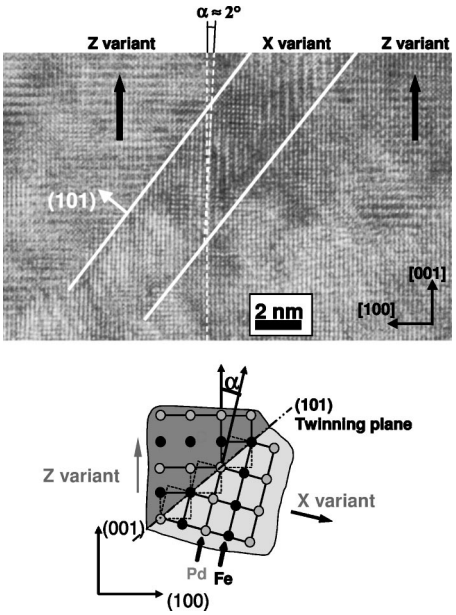

FIG. 5. TEM cross section along (010) (zone axis [010]) on a 40 nm FePd layer annealed at 400 °C for 48 h; high resolution image showing the contrast between Fe and Pd (100) planes in *X*-variant domain, and the twinning of this domain with *Z* variants relatively to (101) planes. The disorientation of the (100) planes in *X* variants is assessed at 2°.

crossing the whole FePd layer, with a tip-terminated end at the bottom of the layer. The fraction of the *X*-variant domains on these cross-section images may be estimated to be 1/8. *Z*-variant domains seem to occupy the rest of the layer, quite homogenously, hence about $\frac{3}{4}$ of the layer, if we suppose $V_x = V_y$. The difference between this 0,75 value and the 0,66 value measured with x-rays lays within the error bar of these techniques.

Antiphase boundaries (APBs) are observed in both types of domains, as thin anisotropic dark lines[13,15,20,21] that correspond to chemically disordered volumes. Furthermore, an interfacial layer of about 8 nm is observed on both types of dark field images at the FePd/Pd interface. We believe these layers to be due to a $L1_2$ ordered zone. Indeed, such ordered structures are expected to induce nonzero intensity on both (100) and (001) superstructure spots with a lower intensity than in the case of the $L1_0$ ordered structure. If this zone had a $L1_0$ structure, it could not be observed on both dark field images: It would appear on only one, with the same intensity as in the upper part. Moreover, high-resolution images clearly show that this interfacial layer has a $L1_2$ structure. This $L1_2$ phase is expected to appear close to the $FePd_3$ composition of the alloy.[12] Its precise chemical composition will be discussed below.

High resolution images performed on the same cross sections (Fig. 5) confirm the presence of $L1_0$ in-plane ordering: They show the alternated vertical dark and bright (100) planes corresponding to Fe and Pd in the $L1_0$ *X* variant. The same contrast may be seen for the horizontal (001) planes in the *Z* variants. The interfaces between an in-plane ordered domain and the adjacent out-of-plane ordered domains lay along parallel (110) planes, forming a twinning plane between the two variants. This twinning interface seems to be coherent, as we do not observe any dislocation along these {110} planes. Moreover, the (100) planes in the *X*-variant domains are not perfectly vertical but tilted of about 2° (Fig. 5). This can be explained by the tetragonalisation of the $L1_0$ cell (Fig. 5): the (101) mirror planes make an angle of $\mathrm{arctg}(a_{a,b}/a_c) = \mathrm{arctg}(3.85/3.71)$ # 46° relative to the (001) direction of Pd, thus leading to the observed misangle close to 2° in the *X*-variant domains. It furthermore may explain the relatively large value obtained for the in-plane lattice parameter in *X* and *Y* domains from in-plane x-ray diffraction measurements (3.76 Å). Indeed we measure with x-rays the sum of the two *X*-related peaks that are out-of-axis of 2° relatively to the [100] scanning direction. Thus, the $\theta-2\theta$ scans are out-of axis for *X*-variant domains and cannot give the right value for their out-of-plane lattice parameter. We therefore cannot trust this 3.76 Å value; this also shows a large error bar in the fit we performed on (200) peaks to extract the *X*-volume ratio.

The configuration of the different variants is made clearer by plane view observations of the ordered domains [Fig. 6(a)]. Dark field images show in-plane ordered domains with a shape corresponding to long rectangles (400–500 nm), and with a width of about 40 nm. This value corresponds to the projection on the surface of the 45° domains observed on cross-section images. The two types of *X* and *Y* variants coexist, forming a kind of grid in the FePd layer [Fig. 6(b)]. These domains appear in dark on (110) dark field (variant *Z*) especially in the thin part of the plane view (where they are not totally covered by the inclined *Z*-variant domains). Each domain stops on a perpendicular one that corresponds to the other in-plane variant. The rest of the layer is ordered with the *Z* variant. Again, APBs are clearly visible in the three types of domains.

In order to evaluate the Fe diffusion in the Pd buffer layer, which is observed by XRD and TEM, we performed electron energy loss spectroscopy (EELS) measurements on the same

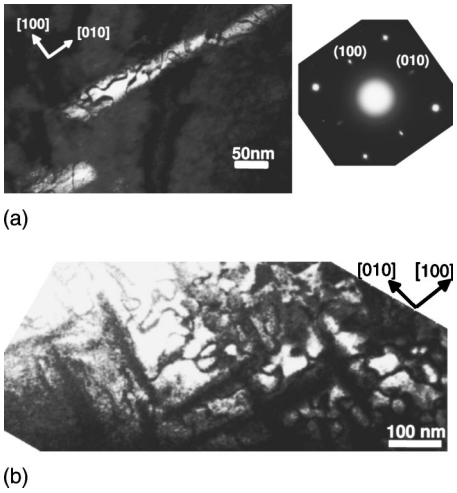

FIG. 6. TEM dark field plane views on a 40 nm FePd layer annealed at 400 °C for 48 h. (a) On (100), showing *X*-variant domains as long (300–400 nm) prisms along (010), with a width in the order of 4–5 nm. APB are clearly visible; the diffractogram confirms the presence of the three $L1_0$ variants [*X* variant with the related (100) spots, *Y* variant with (010), and *Z* variant with (110)] (b) On (110), showing *Z*-variant domains and, in negative (dark), both *X* and *Y* domains, along the (010) and (100) directions. This observation is made possible as the layer is here very thin and *Z* domains do not cover the whole surface on (001) projections. The change in film thickness close to the edge of the film explains the apparent change in *X* domains width.

cross section as shown above. Experiments were performed on a 300 keV JEOL 3010 microscope equipped with a Gatan image filter. With this technique, we can image the spatial distribution of the different chemical species in a film. The chemical map of Iron was obtained on cross sections thanks to the three-window method[22] applied at the L_2L_3 ionization edge of iron at 708 eV (Fig. 7). The Pd concentration map was not recorded due to a large C contamination in the microscope during this experiment: The K edge of C (284 eV) has a strong component that overwhelms the Pd edge at 365 eV. In order to evaluate the Fe and Pd concentration, we assumed that the alloy contained Pd and Fe only, and that the top layer of the alloy was equiatomic. Using these assumptions, the evaluation of the concentrations is straightforward.

These analyses indicate a large stoechiometric zone corresponding to the $Fe_{0.5}Pd_{0.5}$ composition. The thickness of this zone is close to 35 nm, a bit thinner than the initial thickness of the deposited alloy (40 nm). A 20 nm thick layer corresponds to the interface between this region and the pure-Pd buffer layer. In this interfacial zone the Fe content decreases from 0.5 to 0. The rest of the buffer layer does not show a Fe content above the noise of this measurement. The Fe concentration profile can be compared to dark field images of Fig. 4. The L_{12} zone (8 nm in Fig. 4) is found to correspond to a Fe_xPd_{1-x} composition range $0.15<x<0.38$, in perfect agreement with the FePd bulk phase diagram.[12] This observation of the composition range of a given phase in a stressed film is an original result. It gives an indication on the influence of the stress on the stability of the structure. In the case of the cubic L_{12} structure, the stress seems not to modify the composition range, contrary to what was observed for instance in tetragonal chemically ordered structures.[6,21,23]

V. DISCUSSION

The appearance of the three variants of the $L1_0$ structure stresses the differences between ordering during growth or during annealing. It has been claimed that the uniaxial $L1_0$ ordering during codeposition could be induced by the epitaxial tensile stress that favors the *Z* variant.[7] In that case the uniaxialy *Z*-ordered structure would be the equilibrium state of the stressed thin film and we would then observe a similar ordering after annealing. Our results demonstrate that the uniaxial ordering during codeposition above 350 °C is not due to an equilibrium structure but rather to a kinetic process occurring at the surface during growth, the ordered surface structure being "frozen" as the growth is going on.[13] We have to stress that the structure that we obtained after annealing disordered thin films is very close to the structure which has been observed in annealed bulk samples. In this case, the three variants appear in equal proportions and different regions are observed where two domains coexist ($X+Y$, $Y+Z$, or $X+Z$).[24,25] In a given region, the ordered domains appear as alternated periodic lamellar domains twinned with respect to the {110} planes. In our case we also observe the three variants of the $L1_0$ phase forming also a lamellar structure: Domains corresponding to the different variants are twinned

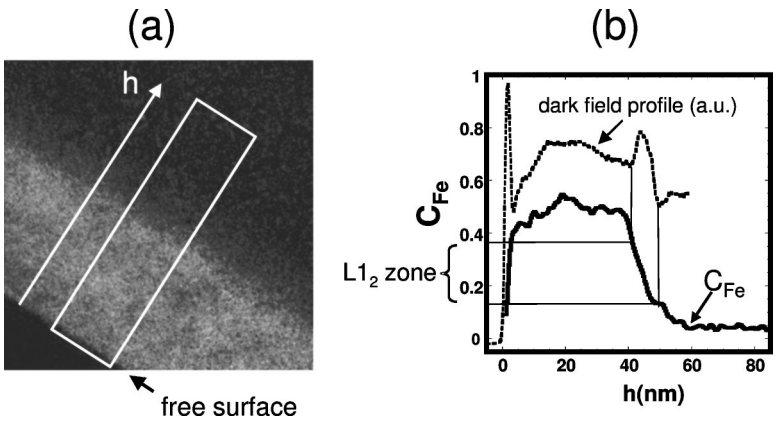

FIG. 7. (a) EELS image [cross section along (010)] on a 40 nm FePd layer annealed at 400 °C for 48 h. The Fe map shows an interdiffusion of the Fe into the buffer, rather than an abrupt interface. (b) The Fe concentration (C_{fe}) profile plot as an average on a given bandwidth [shown in (a)]. It is calculated assuming an equiatomic alloy close to the free surface. As a comparison, we show the profile obtained in Fig. 4 on the (100) dark field, increasing its intensity when crossing the $L1_2$ band.

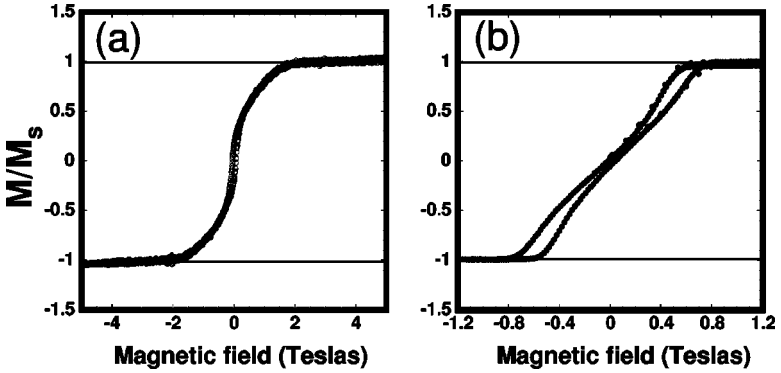

FIG. 8. Hysteresis loops on a 40 nm FePd film, initially disordered and annealed at 400 °C for 48 h. (a) VSM measurement of the in-plane magnetization with H applied in-plane (b) extraordinary Hall effect measurement of the magnetization perpendicular to the film, with H applied perpendicular to the film.

relative to {110} planes that are mirror planes for the tetragonal axis in the two domains. As pointed out above, the interface between domains along a twinning plane seems to be coherent, without dislocations at this interface. Nevertheless some differences relative to the bulk case have to be noticed: The three variants coexist in the same regions, are not paired in given regions and no periodicity of the domains is observed, contrary to the case of bulk samples. The most striking feature is the asymmetry between *Z*-variant domains on the one hand and *X*- or *Y*-variant domains on the other hand: The *Z*-variant dominates (about 2/3 of the FePd volume) whereas in bulk samples the three variants are equally represented. This behavior can be explained by taking into account the influence of stress on the selection of one ordered variant. As we have noticed, no extra dislocations appear at the interface between domains. Moreover, the average in-plane lattice parameter is the same after and before annealing (see Ref. 23 for the in-plane lattice parameter measurements by RHEED on disordered FePd films). So, we can suppose that no new dislocation appears at the FePd/Pd interface during annealing. It thus suggests that the extra strain due to tetragonalization during ordering is accommodated by elastic deformation. Let us consider the average in-plane lattice parameter before annealing: For such a thickness it is close to $a_{\text{initial}}=3.825$ Å.[26] After annealing, the V_x, V_y, and V_z volume of the different variants should follow, in order to keep the same average in-plane lattice parameter: $V_x=V_y$ and $V_x\,(a_{\text{initial}}-a_c)=(V_y+V_z)(a_{a,b}-a_{\text{initial}})$ where $a_c=3.71$ Å and $a_{a,b}=3.85$ Å in the bulk case. From this we obtain $V_z=0.64\,V_{\text{total}}$, that is in good agreement with the evaluated value from XRD and TEM. Residual epitaxial strain in the as-deposited layer thus fixes the proportion of the different variant domains and this, in turn, explains the saturation value observed for the LRO parameter associated with the *Z* variant.

The strong effect of stress on the $L1_0$ ordering has already been put forward in FePt by Ichitsubo[23] on bulk samples: Annealing such alloys under tensile stress favors the $L1_0$ variant having *c* perpendicular to the applied stress. We, in fact, observe exactly the same behavior in our epitaxial FePd layers: The driving force here is due to the residual epitaxial stress.

Finally, a last observation has to be made concerning the shape of *X* or *Y* domains: As may be seen on cross sections (Fig. 4), all of them reach the surface. Some of them cross the whole FePd layer until the $L1_2$ zone, but some of them seem to stop above this zone, and to finish with a tip-ended shape which is not compatible with a perfect twinning between parallel {101} planes. In contrast, *Z* variants seem to be uniformly present in the whole thickness of the FePd film. This indicates either surface-induced ordering for *X* and *Y* variants or non-uniformity of residual epitaxial strain as a function of the depth in the FePd layer. In fact, it has been observed[26] that the $\frac{1}{2}[101]$ dislocations that allow the relaxation of the disordered FePd layer are not at the very interface with the Pd buffer but rather spread above this interface, at different heights. This could explain the higher strain relaxation closer to the surface, and thus a smaller in-plane lattice parameter, favoring larger *X* and *Y* domains volume. Both explanations are not incompatible: Even in *X* and *Y* variants the chemical ordering might originate at the surface and then propagate to the deeper regions of the film. Whatever the kinetic of ordering may be, as we observed the samples (for instance, on the cross section) after a long time (the LRO parameter saturates), the whole film might have reached a kind of equilibrium. We thus cannot expect the *X* and *Y* variants to grow any more toward the deeper regions. So, their particular shape might reflect a real nonuniformity of the strain. It again confirms the influence of the residual strain on the apparition of the different variants.

VI. MAGNETIC MEASUREMENTS

After deposition at room temperature, the FePd films are disordered, and their magnetization lays in the plane of the film due to the demagnetization field.[4,17] Hysteresis loops were measured after a 48 h annealing at 400 °C: The in-plane magnetization along [100] was measured with a vibrating sample magnetometer (VSM), and the perpendicular magnetization by extraordinary Hall effect (Fig. 8). From the difference between these two curves we can deduce a quality factor which corresponds to the ratio of the energy for an in-plane magnetization versus a perpendicular magnetization.[3,4,27] *Q* is found close to 1.25. As it is larger than unity, the magnetization is now perpendicular to the film. This is due to the magnetic anisotropy in the majority $L1_0$ *Z* domains having *c* along [001]. This *Q* value can be compared to the expected value from structural observations: Let us assume for the three ordered variants a local anisotropy coefficient K_u equal to the one observed for well uniaxially ordered layers[4] ($K_u/2\pi M_s^2\approx 2$, where M_s is the FePd saturation magnetization). This assumption is made

consistent by the observation of a LRO parameter close to unity in the different types of domains. If we call V the volume fraction of the FePd layer that orders along [001], the two other variants correspond to a $(1-V)/2$ fraction. Taking into account the demagnetization energy in the case of a perpendicular magnetization $(2\pi M_s^2)$, Q is given by

$$Q = \frac{VK_u + \frac{1-V}{2}K_u}{(1-V)K_u + 2\pi M_s^2} = \frac{V+1}{3-2V}.$$

XRD measurements suggest $V \approx 2/3$, that would yield $Q=1$, slightly lower than the 1.25 measured value. This latest value would correspond to $V=0.75$, equal to the value obtained from dark field images by TEM. So, we can consider that the structural results are clearly consistent with the magnetic results and that our simple model explains the total magnetic anisotropy of the layer.

VII. SUMMARY AND CONCLUSION

We have grown chemically disordered FePd epitaxial layers by MBE on Pd(001) and then annealed them in order to induce the chemically ordered $L1_0$ structure. The long-range order parameter associated with the $L1_0$ variant with c along (001) saturates at a value close to 0.65. Moreover, the ordered structure appears in the three possible variants of the $L1_0$ phase, in domains twinned relatively to $\{101\}$ planes. This is contrary to what is observed in the case of samples ordered during growth. Because of the tetragonalization associated with the $L1_0$ ordering, the ratio of the three different variant volumes is fixed by the residual strain in the layer before annealing, and consequently explains the saturation value of the LRO parameter. A large interdiffusion region at the FePd/Pd interface showed a $L1_2$ chemically ordered structure. We performed both chemical and structural measurements on this $L1_2$ region and proved that it corresponds to the expected stoechiometry from the FePd bulk phase diagram.

The $L1_0$ ordering of the layer leads in our case to a perpendicular magnetization relative to the film plane, due to the magnetic anisotropy of majority Z-ordered domains. Nevertheless, it requires a very long annealing time (more than 10 h), that makes this method not useable for technical applications. The alternative of increasing the annealing temperature to decrease the annealing time might face the problem of a large Fe diffusion into the Pd buffer layer.

As a conclusion, this study of post-growth chemical ordering clearly shows that the $L1_0$ monovariant structure can hardly be reached by an annealing method on initially disordered samples. The epitaxial stress alone does not lead to the selection of the Z variant: We have to favor the creation of Z variants. For this purpose, two methods have been successful up to now: (i) Either we induce during growth small Z-variant domains at low temperature by an alternated Fe and Pd deposition, followed by ion irradiation at low temperature[28] that makes these Z domains occupy the whole FePd layer; (ii) or we can take advantage on the surfactant properties of Pd adatoms as shown in the case of codeposition above 350 °C where the Z variant is selected by this surface diffusion mechanism.[13] The results that we obtained here during annealing contributed to distinguishing between the influence of the dynamics of ordering during growth on a surface, and the influence of epitaxial stress on the equilibrium structure of FePd.

*Corresponding author. Electronic address: halley@drfmc.ceng.cea.fr

[1] R. F. C. Farrow, D. Weller, R. F. Marks, M. F. Toney, S. Horn, G. R. Harp, and A. Cebollada, Appl. Phys. Lett. **69**, 1166 (1996).
[2] V. Gehanno, C. Revenant-Brizard, A. Marty, and B. Gilles, J. Appl. Phys. **84**, 2316 (1998).
[3] V. Gehanno, R. Hoffmann, Y. Samson, A. Marty, and S. Auffret, Eur. Phys. J. B **10**, 457 (1999).
[4] V. Gehanno, A. Marty, B. Gilles, and Y. Samsan, Phys. Rev. B **55**, 12552 (1997).
[5] J. P. Hirth and J. Lothe, *Theory of Dislocations*, 2nd ed. (Wiley & Sons, New York, 1982).
[6] G. Abadias, I. Schuster, A. Marty, and B. Gilles, Phys. Rev. B **61**, 6495 (2000).
[7] M. Dynna, A. Marty, B. Gilles, Y. Samson, and G. Patrat, Acta Mater. **45**, 257 (1997).
[8] L. Barbier, B. Salanon, and A. Loiseau, Phys. Rev. B **50**, 4929 (1994).
[9] E. Legoff, L. Barbier, S. Goapper, A. Loiseau, and B. Salanon, Surf. Sci. **466**, 73 (2000).
[10] O. Ersen, V. Parasote, V. Pierron-Bohnes, M. C. Cadeville, and C. Ulhaq-Bouillet, J. Appl. Phys. **93**, 2987 (2003).
[11] D. W. Moon, Y. H. Ha, Y. Park, J. W. Lee, J. Kim, and S. C. Shin, Appl. Phys. Lett. **79**, 503 (2001).
[12] E. A. Brandes and G. B. Brook, *Smithells Metals Reference Book*, 7th ed. (Butterworth-Heinemann, Oxford, 1997), p. 12.
[13] D. Halley, Y. Samson, A. Marty, C. Beigné, and B. Gilles, Surf. Sci. **481**, 25 (2001).
[14] D. Halley, P. Auric, P. Bayle-Guillemaud, B. Gilles, A. Marty, and D. Jalabert, J. Appl. Phys. **91**, 9757 (2002).
[15] B. Gilles, F. Xu, D. Halley, A. Marty, Y. Samson, and G. Patrat, Mater. Res. Soc. Symp. Proc. **615**, G1,7 (2000).
[16] B. E. Warren, *X-ray Diffraction* (Dover, New York, 1990).
[17] Y. Samson, A. Marty, R. Hoffmann, V. Gehanno, and B. Gilles, J. Appl. Phys. **85**, 4604 (1999).
[18] R. Arenal de la Concha, I. Schuster, D. Halley, A. Marty, and P. Bayle-Guillemaud, J. Phys. IV **12**, Pr6–25 (2002).
[19] P. Eisenberger and W. C. Marra, Phys. Rev. Lett. **46**, 1081 (1981).
[20] J. M. Pénisson, A. Bourret, and Ph. Eurin, Acta Metall. **19**, 1195 (1971).
[21] Y. LeBouar, A. Loiseau, A. Finel, and F. Ducastelle, Phys. Rev. B **61**, 3317 (2000).
[22] F. Hofer, W. Grogger, G. Kothleimer, and P. Warbichler, Ultramicroscopy **67**, 83 (1997).
[23] T. Ichitsubo, M. Nakamoto, K. Tanaka, and M. Koiwa, Mater.

Trans., JIM **39**, 24 (1998).
[24] B. Zhang, and W. A. Soffa, Scr. Metall. Mater. **30**, 683 (1994).
[25] S. Muto, R. Oshima, and F. E. Fujita, Acta Metall. Mater. **38**, 685 (1990).
[26] D. Halley, A. Marty, P. Bayle-Guillemaud, B. Gilles, and Y. Samson (unpublished).
[27] T. Kusuda, S. Honda, and M. Ohkoshi, J. Appl. Phys. **53**, 2328 (1982).
[28] H. Bernas, J. P. Attané, K. H. Heinig, D. Halley, D. Ravelosona, A. Marty, P. Auric, C. Chappert, and Y. Samson, Phys. Rev. Lett. **91**, 077203 (2003).